Atomic-orbital analysis on multi-orbital Fermi surfaces of $BaFe_2As_2$

Masaru Takizawa[1], Hidetoshi Namba[2], Toshiaki Ohta[3], Kenya Ohgushi[4], Fumihiko Matsui[5], and Hiroshi Daimon[5]

1) Research Organization of Science & Engineering, Ritsumeikan University, Kusatsu, Shiga 525-8577, Japan

2) Department of Physical Sciences, Faculty of Science and Engineering, Ritsumeikan University, Kusatsu, Shiga 525-8577, Japan

3) The SR center, Ritsumeikan University, Kusatsu, Shiga 525-8577, Japan

4) Institute for Solid State Physics, University of Tokyo, Kashiwa, Chiba 277-8581, Japan

5) Graduate School of Materials Science, Nara Institute of Science and Technology, Ikoma, Nara 630-0192, Japan

Abstract

We have performed the two-dimensional photoelectron spectroscopy measurements on $BaFe_2As_2$ with linearly polarized synchrotron radiation in order to determine *d* orbital characters of the Fermi surfaces of the iron-based superconductors. By rotating the sample, we have obtained the Fermi surfaces with four-fold symmetry. However, the symmetry-lowered photoelectron intensity angular distribution indicates that the Fermi surface around the Γ(Z) point consists of d_{yz}, d_{zx}, and $d_{3z^2-r^2}$ orbitals.

1. Introduction

Since the discovery of a new high-T_c superconductivity in F-doped LaFeAsO [1], the high-T_c research of these iron pnictides has progressed more explosively than for the cuprates. These new iron-based superconductors have some common properties with the cuprates, such as the layered crystal structures and antiferromagnetic ordering in the parent compounds. And many different families of pnictides have been discovered. For example, based on the similar structure to LaFeAsO, $BaFe_2As_2$ was proposed as a potential new parent compound [2] and indeed showed the superconductivity by hole doping [3]. The ternary iron arsenide $BaFe_2As_2$, with the tetragonal $ThCr_2Si_2$-type structure (space group I4/nmm), contains the layers of edge-sharing $FeAs_{4/4}$ tetrahedra, separated by barium atoms, and exhibits a spin-density wave anomaly at 140 K [2]. In spite of the above-mentioned common properties with the cuprates, iron pnictides show very different electronic structures. Unlike the cuprates, the Fermi surfaces of the iron-based superconductors show a three-dimensional dispersion and are composed of multiple bands and orbitals. For example, angle-resolved photoelectron spectroscopy (ARPES) results on $BaFe_2As_2$ show that the hole-like Fermi surfaces (FSs) around the Brillouin zone (BZ) center (Γ point) has strong modulation along the k_z direction, whereas the electron-like FSs around BZ corner (X point) is almost cylinder-like with weak k_z modulation [4]. For the electron-doped $BaFe_2As_2$, orbital characters of the multibands have been reported by the polarization dependent ARPES study, pointing out the inadequacy of the band structure calculations [5]. However, the conventional polarization dependent ARPES tells us only even or odd symmetry of the initial state. On the other hand, a two-dimensional photoelectron intensity angular distribution (PIAD) obtained by using a polarized synchrotron radiation (SR) and a two-dimensional display-type spherical mirror analyzer (DIANA) [6] can resolve the atomic orbitals [7]. For example, two-dimensional photoelectron spectroscopy (2D-PES) measurements on Cu with linearly polarized SR have revealed that the FS of Cu is composed of mainly 4*p* orbitals with their axes pointing outward [8]. In this work, we have performed the 2D-PES measurements on the parent compound of $BaFe_2As_2$ with linearly polarized SR light in order to determine the *d* orbital character.

2. Experimental

The experiment was performed at the linearly polarized soft x-ray beamline BL-7 of SR center, Ritsumeikan University [9]. The electric vector of the linearly polarized SR light was in the horizontal plane and incident on the sample normal. The single crystals of $BaFe_2As_2$ were grown by the self-flux method [10]. The $BaFe_2As_2$ single crystal sample

was cleaved *in situ* in an ultrahigh-vacuum chamber to obtain a clean surface. The surface quality was checked by low energy electron diffraction measurement, showing 1×1 spots. The 2D-PES measurements were performed at room temperature under ultrahigh vacuum of ~ 1×10^{-8} Pa using DIANA [6, 11] with SR light. A 2D-PIAD and a stereo profile of the FS are efficiently obtained by using DIANA. 2D-PIADs of this experiment were collected by energy window of 300 meV. Typical acquisition time for one PIAD was 30 sec. The photon energy was set to about 46.5 eV in order to trace the Γ plane in the three-dimensional BZ. The total energy resolution was about 600 meV. The angular resolution was about 1◦.

3. **Results**

Figure 1 (a) shows the angle-integrated spectrum of $BaFe_2As_2$ taken with $h\nu$ = 46.5 eV. As the previous works on the other iron pnictides [12], the Fe 3*d* derived sharp peak appears at the Fermi level. As shown in Fig. 1(b), the PIAD pattern near the Fermi level shows strong intensity near Γ(Z) and X points, which correspond to the hole-like FSs near the Γ point and

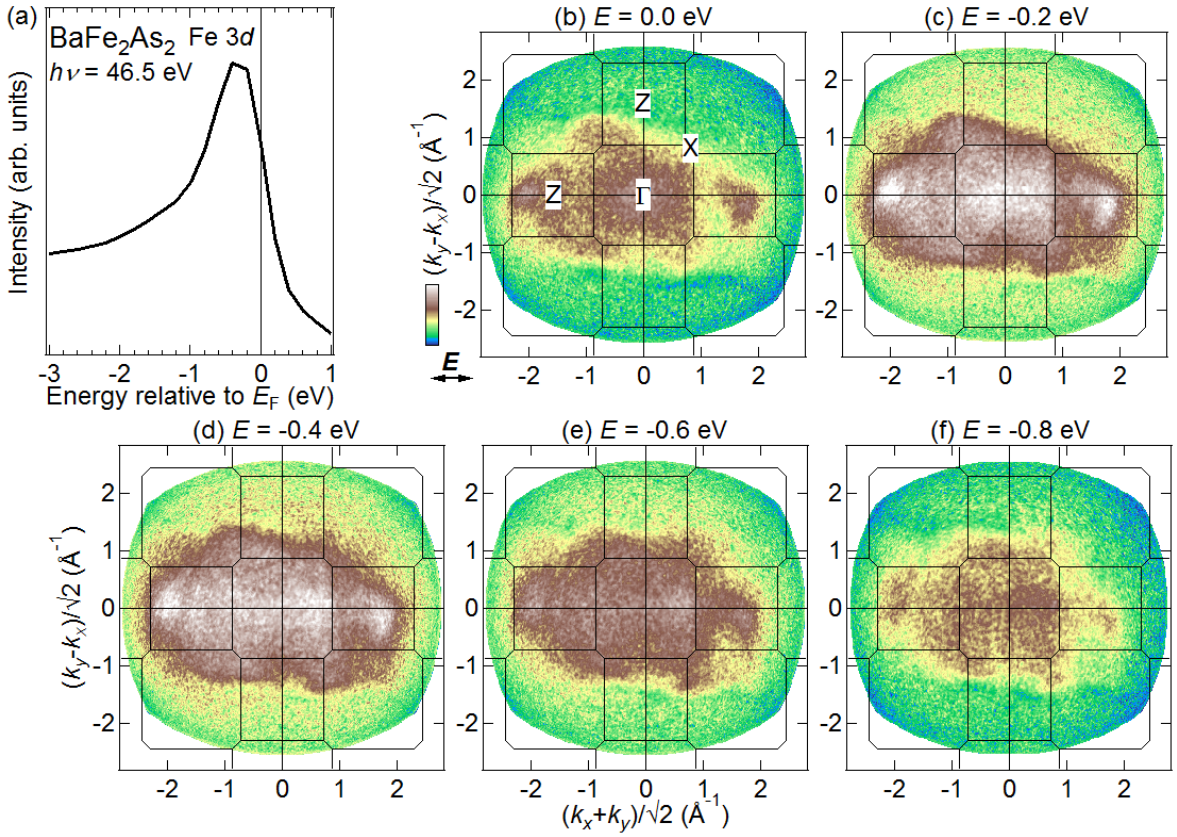

Fig. 1 2D-PES result of $BaFe_2As_2$ taken with $h\nu$ = 46.5 eV. (a) Angle-integrated PES spectrum. The PIADs at E = 0.0 eV (b), -0.2 eV (c), -0.4 eV (d), -0.6 eV (e), and -0.8 eV (f). Solid lines indicate the Γ plane in the three-dimensional BZ. Some symmetry points are depicted in (b). The electric vector of the incident light is in the horizontal direction.

the electron-like FSs near the X point [4]. As shown in Fig. 1(b)-(f), the series of PIAD change with energy, reflecting the band dispersion of Fe 3*d*. With decreasing the energy, the Fe 3*d* state at Γ(Z) point becomes weakened below ~ -0.6 eV. This observation is also consistent with the fact that the Fe 3*d* bands around Γ point have a gap below ~ -0.6 eV [5]. However, the symmetry of the PIAD pattern was different from the expected one with a four-fold symmetry due to the tetragonal crystal structure of $BaFe_2As_2$ [2]. This is due to the matrix element effect of the incident linearly polarized SR light. This effect is discussed below. By rotating the sample around the surface normal (*c*-axis), the angle-dependent PIADs near the Fermi level were obtained. As shown in Fig. 2, the PIADs rotates clockwise with increasing the azimuth angle ϕ. The PIADs of ϕ = 90° and ϕ = 135° are similar to those of ϕ = 0° and ϕ = 45°, respectively. This indicates that the measured electronic

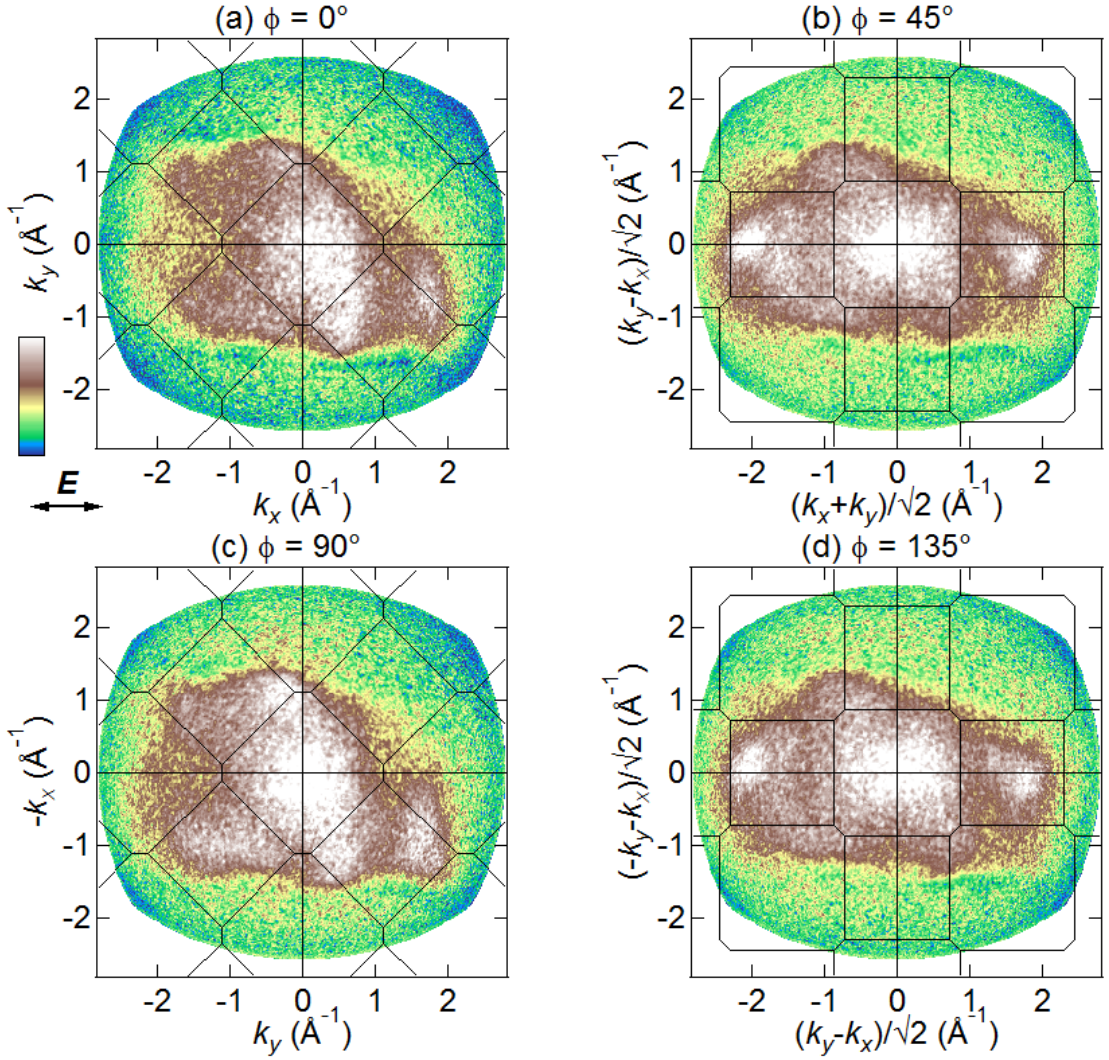

Fig. 2 Angle-dependent PIADs at the Fermi level (*E* = 0.0 eV) taken with *h*ν = 46.5 eV. The PIADs of ϕ = 0° (a), 45° (b), 90° (c), and 135° (d). Solid lines indicate the Γ plane in the three-dimensional BZ. The electric vector of the incident light is in the horizontal direction.

structure indeed has a four-fold symmetry due to the tetragonal crystal structure of $BaFe_2As_2$ [2].

4. Discussion

The analysis of two-dimensional PIAD from a tight-binding approximated valence band and a Bloch-wave final state showed that the photoelectron intensity $I(\theta_k, \phi_k)$ in the direction of polar angle θ_k and azimuth angle ϕ_k can be expressed as [8, 13]:

$$I(\theta_k, \phi_k) \sim D^1(k_{//}) \, |\Sigma_\nu A_\nu|^2,$$

where $D^1(k_{//})$ is the one-dimensional density of states [14] and A_ν is the "angular distribution from the ν-th atomic orbital" [15].

First, the $D^1(k_{//})$ was obtained using the five band tight binding calculation [16]. As shown in Fig. 3, the calculated FS (small enough energy window of 10 meV) [Fig. 3(a)] well reproduces both the previous experimental and theoretical results [4, 5, 16] while the simulated FS [Fig. 3(b)] for this experimental condition seems very different because of the finite energy window of 300 meV. Nevertheless, the strong intensity around Γ point is the same feature for both the simulated and the experimental FSs. Therefore, we can compare the experimental FS with this simulated FS around Γ point.

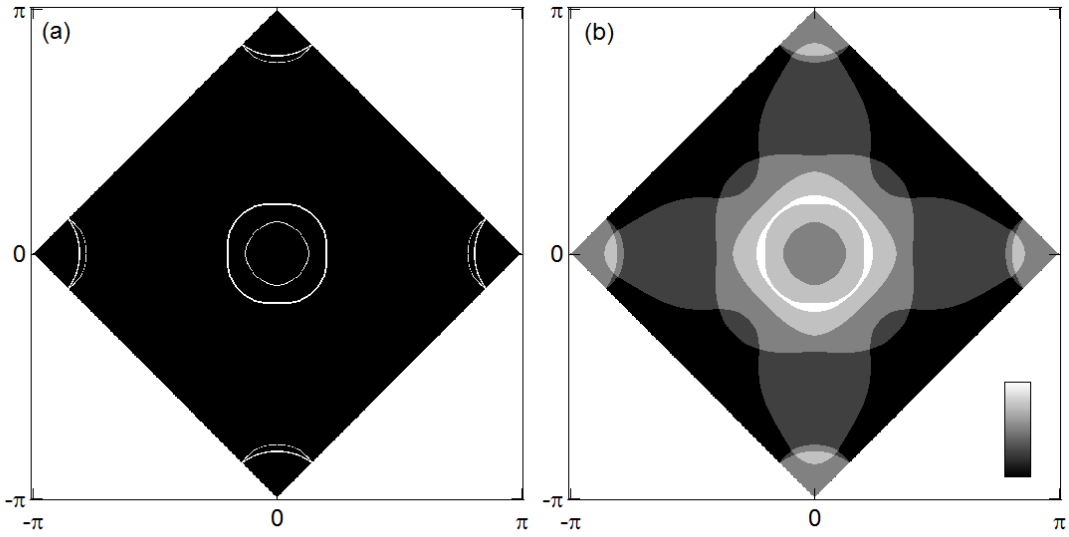

Fig. 3 Calculated Fermi surfaces for $BaFe_2As_2$. Energy window is set to 10 meV (a) and 300 meV as the same condition as this experiment (b).

Next, the $|A_\nu|^2$ from each *d* orbital was calculated according to Ref. [15]. As shown in Fig. 4, the angular distribution from an atomic orbital is not uniform but unique to the atomic orbital due to the relation between the polarization vector of the incident SR and the atomic

orbital. Therefore, comparing the experimental PIAD with these angular distributions from the atomic orbitals, one can determined the atomic orbitals constituting the FS. Here it should be noted that the angular distribution from d_{zx} orbital for $\phi = 90°$ is the same as that from d_{yz} orbital for $\phi = 0°$ and vice versa.

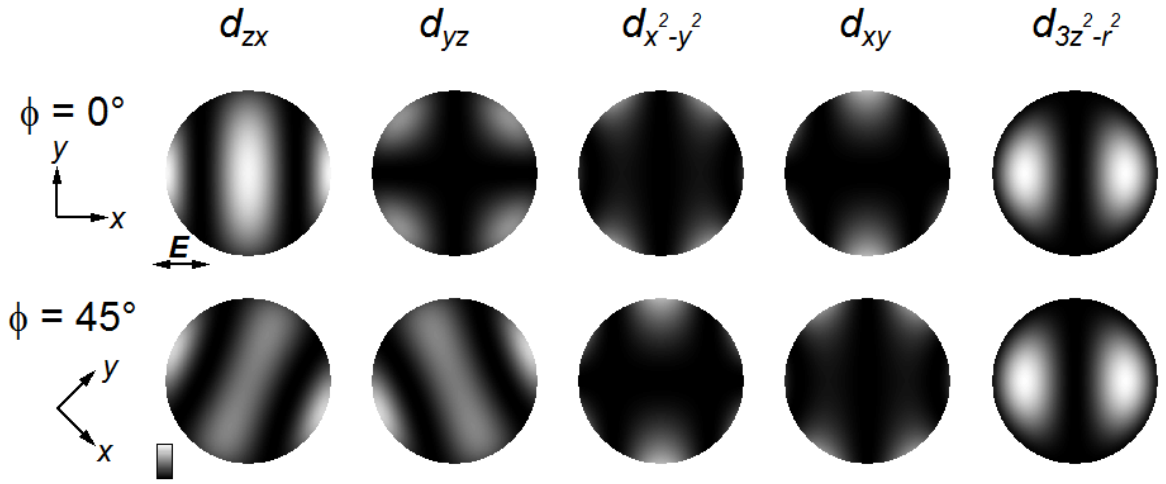

Fig. 4 Calculated angular distributions from each *d* atomic orbital for $\phi = 0°$ and 45° [16].

By multiplying the $D^1(k_{//})$ [Fig. 3] and the $|A_v|^2$ [Fig. 4], simulated PIADs for the $BaFe_2As_2$ FS taken with $h\nu$ = 46.5 eV are obtained [Fig. 5]. Here, the work function of the sample is assumed to be 4.5 eV. For $\phi = 0°$ (90°), the prominent feature around the center (0 $Å^{-1}$, 0 $Å^{-1}$) comes from d_{zx} (d_{yz}) orbital and the features around (±1 $Å^{-1}$, ±1 $Å^{-1}$) and (±2.2 $Å^{-1}$, 0 $Å^{-1}$) are due to $d_{3z^2-r^2}$ orbital. For $\phi = 45°$ (135°), the prominent features around (±1.6 $Å^{-1}$, 0 $Å^{-1}$) comes from $d_{3z^2-r^2}$ orbital and the weak feature around the center (0 $Å^{-1}$, 0 $Å^{-1}$) is due to

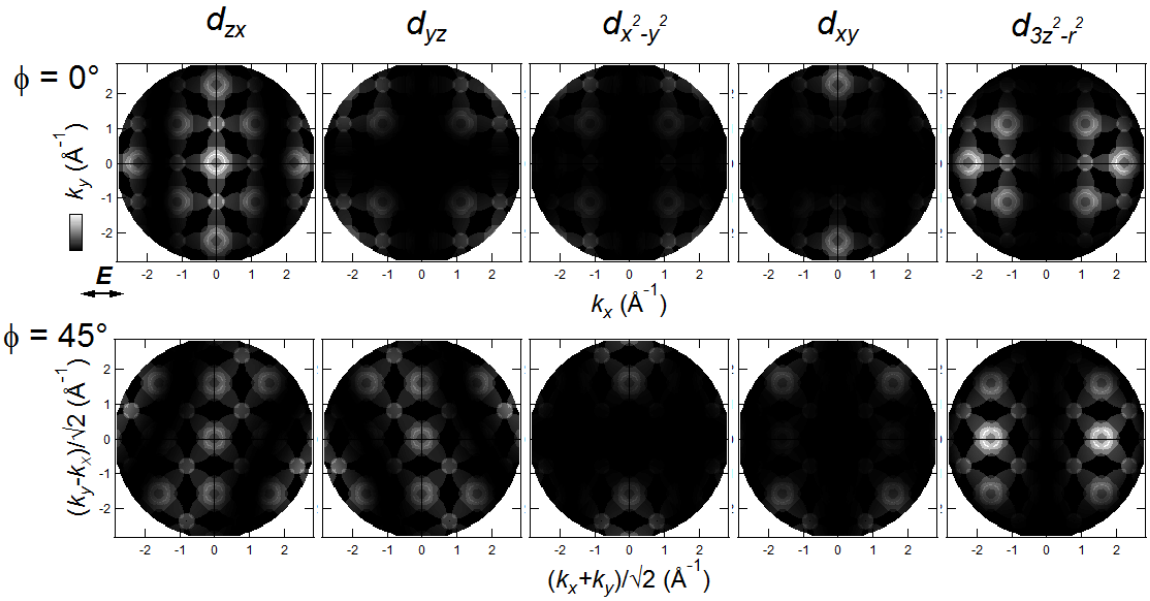

Fig. 5 Simulated PIADs for the $BaFe_2As_2$ FS taken with $h\nu$ = 46.5 eV. The FS is assumed to be composed of each *d* atomic orbital for $\phi = 0°$ and 45°.

both d_{zx} and d_{yz} orbitals. As shown in Fig. 2, the experimental FS shows strong structures around the center (0 $Å^{-1}$, 0 $Å^{-1}$) independent of the angle ϕ, indicating that the d_{zx} and d_{yz} orbital components are necessary to reproduce these experimental results. Furthermore, strong structures around (±1.8 $Å^{-1}$, 0 $Å^{-1}$) observed for ϕ = 45° (135°) suggest that $d_{3z^2-r^2}$ orbital component is also needed. This is also confirmed by the weak structures observed around (±1 $Å^{-1}$, ±1 $Å^{-1}$) for ϕ = 0° (90°), though the lack of intensities around (1 $Å^{-1}$, 1 $Å^{-1}$) and (±2.2 $Å^{-1}$, 0 $Å^{-1}$) may be due to the experimental apparatus problem and the proximity to the detector periphery, respectively.

5. Conclusions

We have performed two-dimensional photoelectron spectroscopy measurements on $BaFe_2As_2$. We have observed the $BaFe_2As_2$ Fermi surface which has a four-fold symmetry due to the tetragonal crystal structure of $BaFe_2As_2$. The photoelectron intensity angular distribution (PIAD), however, showed symmetry-lowered pattern due to the relation between the polarization vector of the incident synchrotron radiation and the atomic orbitals constituting the $BaFe_2As_2$ Fermi surface. Compared with the simulated PIADs from the atomic orbitals, it is suggested that the $BaFe_2As_2$ Fermi surface around the Γ(Z) point is constituted by d_{yz}, d_{zx}, and $d_{3z^2-r^2}$ orbital components.

Acknowledgement

This work was partly supported by Open Advanced Research Facilities Initiative.

References

[1] Y. Kamihara, T. Watanabe, M. Hirano, and H. Hosono, J. Am. Chme. Soc. **130**, 3296 (2008).

[2] M. Rotter, M. Tegel, D. Johrendt, I. Shellenberg, W. Hermes, R. Pöttgen, Phys. Rev. B **78**, 020503(R) (2008).

[3] M. Rotter, M. Tegel, and D. Johrendt, Phys. Rev. Lett. **101**, 107006 (2008).

[4] W. Malaeb, T. Yoshida, A. Fujimori, M. Kubota, K. Ono, K. Kihou, P. M. Shirage, H. Kito, A. Iyo, H. Eisaki, Y. Nakajima, T. Tamegai, and R. Arita, J. Phys. Soc,. Jpn. **78**, 123706 (2009).

[5] Y. Zhang, F. Chen, C. He, B. Zhou, B. P. Xie, C. Fang, W. F. Tsai, X. H. Chen, H. Hayashi, J. Jiang, H. Iwasawa, K. Shimada, H. Namatame, M. Taniguchi, J. P. Hu, and D. L.

Feng, Phys. Rev. B **83**, 054510 (2011).
[6] H. Daimon, Rev. Sci. Instrum. **59**, 545 (1988).
[7] H. Daimon, M. Kotsugi, K. Nakatsuji, T. Okuda, and K. Hattori, Surf. Sci. **438**, 214 (1999).
[8] F. Matsui, H. Miyata, O. Rader, Y. Hamada, Y. Nakamura, K. Nakanishi, K. Ogawa, H. Namba, and H. Daimon, Phys. Rev. B **72**, 195417 (2005).
[9] Y. Hamada, F. Matsui, Y. Nozawa, K. Nakanishi, M. Nanpei, K. Ogawa, S. Shigenai, N. Takahashi, H. Daimon, and H. Namba, AIP Conf. Proc. **879**, 547 (2007).
[10] K. Ohgushi and Y. Kiuchi, Phys. Rev. B **85**, 064522 (2012).
[11] N. Takahashi, F. Matsui, H. Matsuda, Y. Hamada, K. Nakanishi, H. Namba, and H. Daimon, J. Electron Spectrosc. Relat. Phenom. **163**, 45 (2008).
[12] W. Malaeb, T. Yoshida, T. Kataoka, A. Fujimori, M. Kubota, K. Ono, H. Usui, K. Kuroki, R. Arita, H. Aoki, Y. Kamihara, M. Hirano, and H. Hosono, J. Phys. Soc. Jpn. **77**, 093714 (2008).
[13] H. Daimon, S. Imada, H. Nishimoto, and S. Suga, J. Electron Spectrosc. Relat. Phenom. **76**, 487 (1995).
[14] T. Grandke, L. Ley, and M. Cardona, Phys. Rev. B **18**, 3847 (1978).
[15] S. Goldberg, C. Fadley, and S. Kono, J. Electron Spectrosc. Relat. Phenom. **21**, 285 (1981).
[16] S. Graser, T. A. Maier, P. J. Hirschfeld, and D. J. Scalapino, New J. Phys. **11**, 025016 (2009).